

**Featuring work from the Biomedical Sensing Systems Laboratory,  
Prof. Weihua Guan, The Pennsylvania State University, USA**

**A field-deployable mobile molecular diagnostic system for malaria  
at the point of need**

Field-deployable, standalone, sample-in-answer-out molecular diagnostic system (AnyMDx) to enable real-time molecular analysis of blood-born malaria at the point of need. The AnyMDx seamlessly integrates all nucleic acid testing steps from sample preparation to real-time amplification and detection. The turnaround time from raw sample to answer is less than 40 minutes.

**As featured in:**



See Weihua Guan et al., *Lab Chip*,  
2016, 16, 4341.



[www.rsc.org/loc](http://www.rsc.org/loc)

Registered charity number: 207890


 Cite this: *Lab Chip*, 2016, 16, 4341

## A field-deployable mobile molecular diagnostic system for malaria at the point of need†

 Gihoon Choi,<sup>a</sup> Daniel Song,<sup>b</sup> Sony Shrestha,<sup>c</sup> Jun Miao,<sup>c</sup>  
 Liwang Cui<sup>c</sup> and Weihua Guan<sup>\*ab</sup>

In response to the urgent need of a field-deployable and highly sensitive malaria diagnosis, we developed a standalone, “sample-in-answer-out” molecular diagnostic system (AnyMDx) to enable quantitative molecular analysis of blood-borne malaria in low resource areas. The system consists of a durable battery-powered analyzer and a disposable microfluidic compact disc loaded with reagents ready for use. A low power thermal module and a novel fluorescence-sensing module are integrated into the analyzer for real-time monitoring of loop-mediated isothermal nucleic acid amplification (LAMP) of target parasite DNA. With 10  $\mu\text{L}$  of raw blood sample, the AnyMDx system automates the nucleic acid sample preparation and subsequent LAMP and real-time detection. Under laboratory conditions with whole-blood samples spiked with cultured *Plasmodium falciparum*, we achieved a detection limit of  $\sim 0.6$  parasite per  $\mu\text{L}$ , much lower than those for the conventional microscopy and rapid diagnostic tests ( $\sim 50$ – $100$  parasites per  $\mu\text{L}$ ). The turnaround time from sample to answer is less than 40 minutes. The AnyMDx is user-friendly requiring minimal technological training. The analyzer and the disposable reagent compact discs are cost-effective, making AnyMDx a potential tool for malaria molecular diagnosis under field settings for malaria elimination.

 Received 26th August 2016,  
 Accepted 28th September 2016

DOI: 10.1039/c6lc01078d

[www.rsc.org/loc](http://www.rsc.org/loc)

## 1 Introduction

Malaria, a mosquito-borne parasitic disease, has been one of the oldest fatal infectious diseases in human history.<sup>1–4</sup> Despite extensive malaria control efforts, it still infects  $\sim 250$  million people in the world per year with the remaining half of the world's population at risk.<sup>3,4</sup> For malaria control, rapid, accurate and highly sensitive diagnosis is essential for delivering effective chemotherapies. Currently, malaria diagnosis under field settings relies exclusively on traditional microscopy and rapid diagnostic tests (RDTs) with a detection limit of 50–100 parasites per  $\mu\text{L}$ .<sup>5–8</sup> Such a detection limit would inevitably miss malaria cases with much lower parasitemias, which are especially common in asymptomatic parasite carriers.<sup>9–12</sup> Thus, malaria diagnostic tools with significantly improved sensitivity are urgently needed for endemic settings, especially for regions planning for malaria elimination.

Modern nucleic acid testing (NAT) methods of malaria detection enable much higher sensitivity with a detection limit

of approximately 1 parasite per  $\mu\text{L}$ ,<sup>8,12</sup> which is highly desirable for identifying asymptomatic infections.<sup>5,6,9,12,13</sup> Sensitive detections of malaria parasites in these subpopulations, which are considered as important reservoirs of transmission, are particularly important for malaria elimination.<sup>2,12</sup> Among various molecular amplification assays, loop-mediated isothermal DNA amplification (LAMP) has emerged as a promising technology for field use due to its simplicity, rapidness, sensitivity and specificity.<sup>5,8,9,14–16</sup> The major advantages of using LAMP include its high specificity, robustness against inhibitors, and fast amplification.<sup>17–19</sup> Unfortunately, most LAMP-based diagnosis still involves bulky and costly peripheral equipment, and skilled technicians are often required for manually operating the instrument<sup>8</sup> and performing multiple steps of sample preparation.<sup>20–23</sup> Moreover, basic infrastructures such as electricity for powering instruments are often limited in remote malaria clinical settings.<sup>24–26</sup> Therefore, there is a strong desire to develop a molecular diagnostic system that can be more easily deployed to remote malaria endemic areas. Although extensive efforts have been undertaken towards this goal,<sup>27,28</sup> a true “sample-in-answer-out” NAT system with real-time quantitative capability has yet to be developed.

A field-deployable molecular malaria diagnostic platform should possess the following attributes: i) standalone and portable for field applications, ii) true sample-in-answer-out without much user intervention, iii) seamlessly integrated

<sup>a</sup> Department of Electrical Engineering, Pennsylvania State University, University Park, 16802, USA. E-mail: w.guan@psu.edu

<sup>b</sup> Department of Biomedical Engineering, Pennsylvania State University, University Park, 16802, USA

<sup>c</sup> Department of Entomology, Pennsylvania State University, University Park, 16802, USA

† Electronic supplementary information (ESI) available. See DOI: 10.1039/c6lc01078d



and automated DNA sample preparation, iv) real-time quantitative fluorescence detection, v) rapid and suitable for diagnosis in clinical settings, and vi) much higher sensitivity allowing detection at low parasitemias. Here, we report the design of a molecular diagnostic system for malaria, named AnyMDx, which consists of a small-footprint analyzer and disposable microfluidic compact discs that are preloaded with molecular reagents for the LAMP assay. With minimal manual work, the AnyMDx could deliver sensitive molecular diagnostic results directly from a small volume of blood samples within 40 minutes without any requirement of laboratory infrastructures. The standalone and user-friendly AnyMDx instrument is highly promising for sensitive malaria diagnosis in field settings.

## 2 Materials and methods

### 2.1 Culture of malaria-infected blood

*P. falciparum* 3D7 was maintained in complete RPMI 1640 medium with type O+ human red blood cells (RBCs) as described previously.<sup>29,30</sup> The parasite culture was synchronized by treatment of ring-stage parasites with 5% D-sorbitol.<sup>31</sup> The fresh complete medium was replaced on a daily basis, and parasitemia was assessed by Giemsa-stained blood smears. In order to mimic the whole blood sample obtained from patients, the parasite culture at the ring stage of various parasitemias was adjusted to around 45% hematocrit for AnyMDx analysis.

### 2.2 AnyMDx instrumentation

The assembled and exploded views of the AnyMDx system are shown in Fig. 1. The instrument was designed in SolidWorks and can be quickly prototyped in-house with a 3D printer.

The whole system is of a small footprint ( $12 \times 13 \times 13$  cm). It is powered by a rechargeable lithium-ion battery allowing for 14 hours of continuous operation before recharging. The functional modules inside the AnyMDx system are illustrated in the block diagram (Fig. 2).

**Real-time optical subsystem.** On the excitation side, the LED light source ( $\lambda = 488$  nm, C503B-BCN-CV0Z0461, Newark) was guided towards the reaction chamber through a polymer optical fiber (#02-538, Edmund). The optical fiber and LED were self-aligned by a customized adapter to achieve optimal light coupling efficiency. On the detection side, the emission light from the LAMP reaction chamber was coupled to the optical sensor (TCS34725, Digi-Key) by the optical fiber. The incidence of the excitation LED light is perpendicular to the optical sensor to minimize the diffracted excitation light into the optical sensor and thus increasing the signal-to-noise ratio.

**Thermal subsystem.** For the feedback thermal control system, a Peltier heater was bonded to the backside of the aluminum heating plate by thermal paste. A micro-thermistor was embedded inside the aluminum heating plate for real-time temperature monitoring. The desired reaction temperature was maintained by the feedback control during the DNA amplification process.

**Mechanical and interfacing subsystems.** An embedded microcontroller unit (MCU) operates the whole system to perform all required isothermal assay steps including automated sample preparation, nucleic acid amplification, and real-time detection. An LCD provides a user-friendly interface for instrument status and data display. In addition, a low power Bluetooth module was incorporated for easy data connectivity.

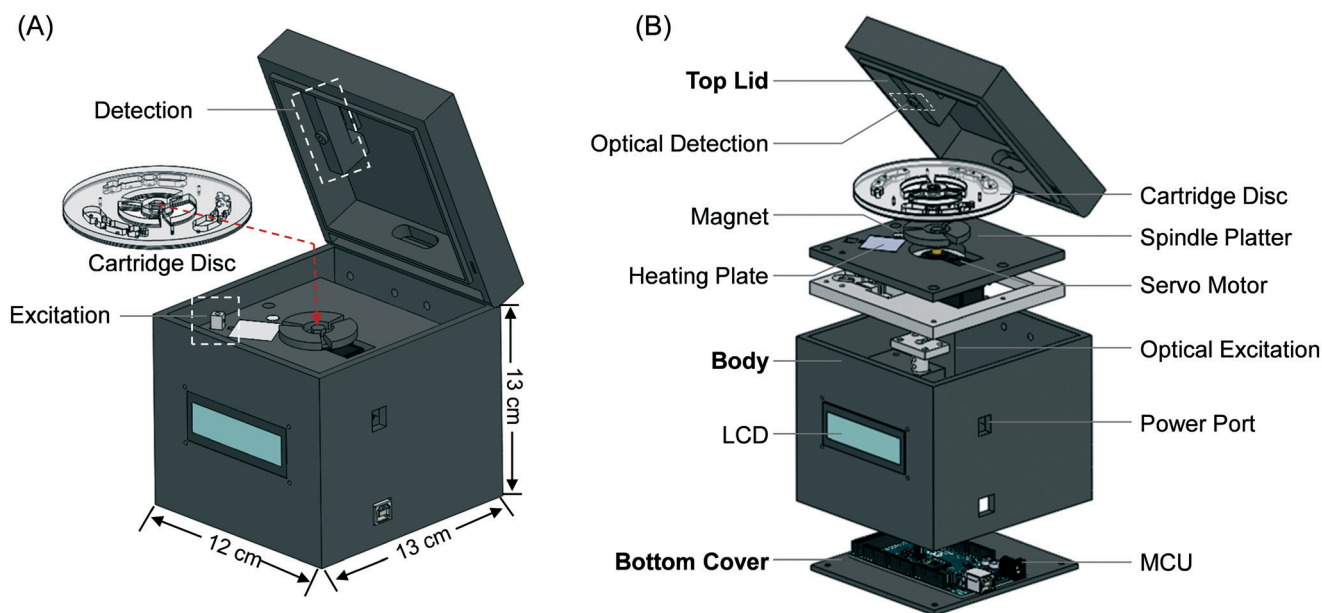


**Fig. 1** Overview of the standalone and mobile nucleic acid testing system (AnyMDx). (A) Schematic diagram of the assembled AnyMDx with the reagent compact disc. The whole platform is of a small footprint ( $12 \times 13 \times 13$  cm). The reagent compact disc was secured on the rotatable spindle platter. (B) Schematic diagram of functional parts in an exploded view.

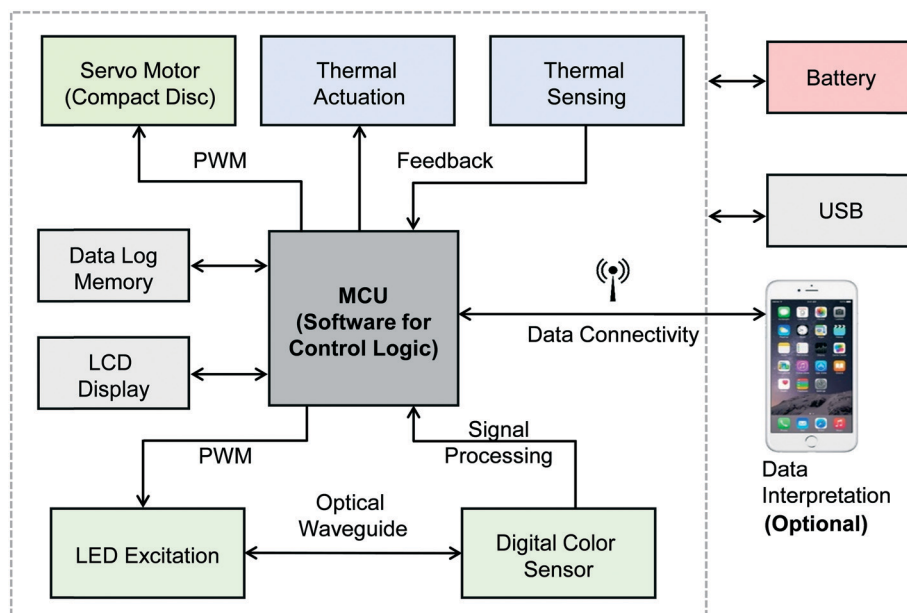


Fig. 2 Block diagram of the AnyMDx modules. The platform consists of four main functional modules: mechanical modules (servo motor/spindle platter/compact disc), optical modules (LED/optical sensor), thermal modules (Peltier heater/thermal sensor), and data connectivity modules (Bluetooth). Each module was controlled by a microprocessor on a customized PCB board. The diagnostic results can be optionally reported to a smartphone user interface.

### 2.3 Microfluidic reagent compact disc design and fabrication

The microfluidic compact disc consists of top (0.8 mm thick), spacer (1.6 mm thick), and bottom (0.8 mm thick) poly(methyl methacrylate) (PMMA) layers laminated with adhesive solvent (Fig. 3A). Each layer was designed in AutoCAD (diameter of 9.6 cm) and patterned by a CO<sub>2</sub> laser cutter (Epilog Helix 24 Laser System). Each assembled disc accommodates three independent testing units. Each unit consists of five chambers: a DNA binding chamber (with an inlet for sample input), a washing chamber, a reaction chamber, and two valving chambers (Fig. 3B). The valving chambers were filled with FC-40 oil or air. The FC-40 oil, which seals the LAMP reaction chamber, helped prevent master mix evaporation during the thermal process. The air-filled valve was surface treated with water-oil repellent to create a barrier for the amphiphilic lysis buffer. The inlets for sample input were sealed by pressure-sensitive adhesive (PSA) tapes (3M Scotch 3650).

### 2.4 Integrated nucleic acid sample preparation on the compact disc

We used a commercially available DNA purification kit (Invitrogen ChargeSwitch® forensic DNA purification kit) for isolating *P. falciparum* DNA from whole blood lysates. The lysis buffer, binding buffer, and washing buffer were used as received. The LAMP master mix was prepared before running the experiments. All reagents were in liquid phase when loaded onto the disc. The reagent-loaded disc were stored in the fridge at 4 °C. The reagents were stable for at least 3 days under these storage conditions. 10 µL of human whole blood samples spiked with cultured *P. falciparum* were collected

into a 1.5 mL microcentrifuge tube containing 1000 µL of lysis buffer and 10 µL of proteinase K. After incubating at room temperature for 2 min, 180 µL of lysates were introduced into the binding chamber through the inlet hole. There are three independent testing units on the compact disc. Each testing unit on the compact disc consists of (1) 30 µL of binding buffer and 10 µL of magnetic beads in the binding chamber, (2) 150 µL of washing buffer in the washing chamber, and (3) 25 µL of LAMP master mix in the reaction chamber (Fig. 3B). Since the surface charge polarity of the magnetic beads is pH dependent and the surface charge polarity of DNA is negative for a wide range of pH values,<sup>32</sup> the magnetic beads can attract or repel the nucleic acids by the different pH values of the preloaded buffer solution (Fig. 3C). The magnetic beads were actuated by rotating the compact disc against a stationary magnet. In a control sequence, the DNA-carrying beads were directed into the different chambers until the target DNA was eluted in the reaction chamber (Fig. 3C). The optimal rotation speed is experimentally determined by monitoring the magnetic bead motion. Although a faster rotation is preferred to reduce the whole processing time, the DNA-carrying magnetic beads might be lost from chamber to chamber if the rotation speed is too high. There is a tradeoff between the sample preparation efficiency and the whole process time. The whole process can automatically prepare high-quality DNA samples from the human whole blood in less than 10 minutes.

### 2.5 Loop-mediated isothermal DNA amplification

The LAMP reaction mix consists of isothermal buffer (20 mM Tris-HCl, 10 mM (NH<sub>4</sub>)<sub>2</sub>SO<sub>4</sub>, 50 mM KCl, 2 mM MgSO<sub>4</sub>, 0.1%

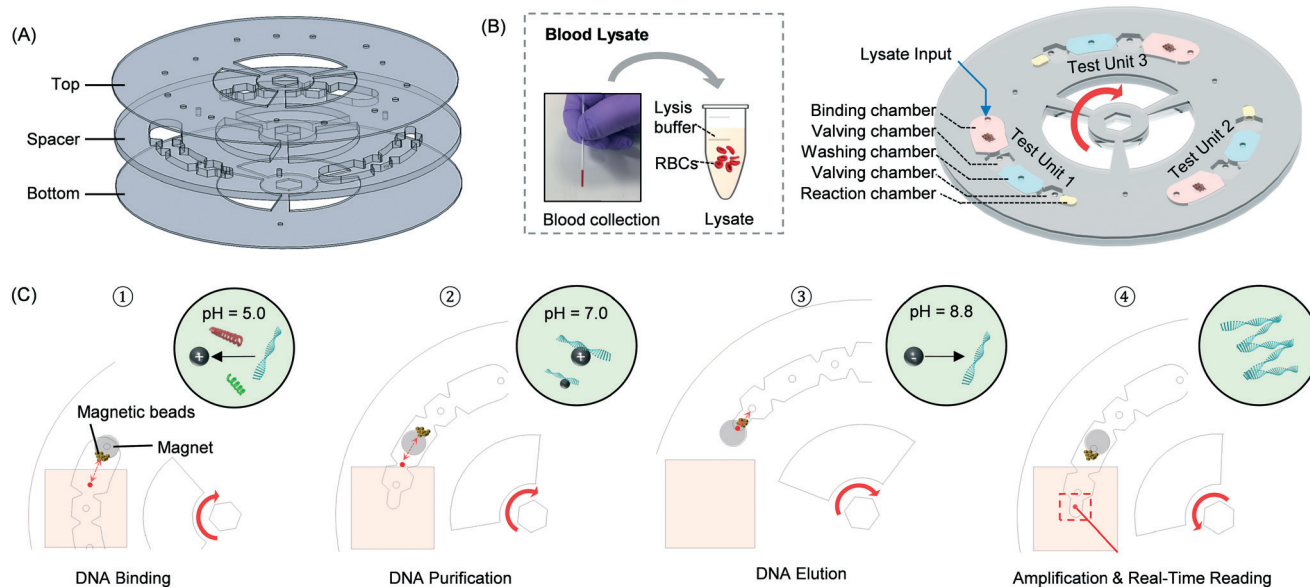


**Fig. 3** Illustration of reagent compact disc and integrated sample preparation on the compact disc. (A) Exploded view of the reagent compact disc showing three patterned PMMA layers. (B) Assembled view of the reagent compact disc showing three independent testing units. Each test unit consists of five chambers: a DNA binding chamber (binding buffer, pH 5.0), a washing chamber (washing buffer, pH 7.0), a LAMP reaction chamber (master mix, pH 8.8), and two valving chambers. All reagents are preloaded on the compact disc in a ready-to-use format. The lysate was prepared by collecting 10  $\mu\text{L}$  of malaria-infected blood into 1 mL of lysis buffer in a microcentrifuge tube. (C) Illustration of integrated sample preparation and amplification steps on the compact disc. By rotating the compact disc against a stationary magnet in a specifically designed control sequence (steps 1–4), the pH charge switchable magnetic beads were directed from chamber to chamber, which allows for seamlessly integrated DNA binding, purification, elution and amplification on the compact disc.

Tween 20, pH 8.8), *P. falciparum*-specific primer set (5 pmol of F3 and B3, 40 pmol of FIP and BIP, 20 pmol of LF and LB, Table S1†),  $\text{MgSO}_4$ , calcein,  $\text{MnCl}_2$ , deoxyribonucleotide triphosphates (dNTPs), *Bst* 2.0 DNA polymerase, DNA template, and PCR grade  $\text{H}_2\text{O}$  (Table 1). The LAMP assay was performed at a constant temperature (65 °C maintained by the analyzer) (Fig. S1†). Six target-specific primers targeting the mitochondrial gene were synthesized (Integrated DNA Technologies) to specifically amplify the 213 bp region of the *P. falciparum* DNA (Fig. 4 and Table S1†). The primer set we used in this study is the same as those reported previously.<sup>15</sup>

## 2.6 Data analysis

During the amplification process, the fluorescence readings were acquired every 2.5 seconds. The first 5 min of the signal was averaged to obtain the background noise level, which was then subtracted from the raw fluorescence readings to

form a processed signal. The processed signal was further smoothed by averaging a fixed number of consecutive data points. We defined threshold time ( $T_t$ ) as the time when the slope of the measured RFU ( $\text{dRFU}/\text{dt}$ ) reached the peak (Fig. S2†). The threshold RFU value was experimentally determined at 400 for positive/negative decision.

## 3 Results and discussion

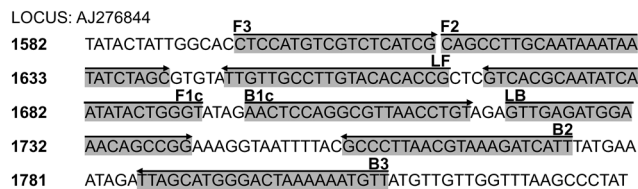
### 3.1 AnyMDx operation

Fig. 5 shows the operation of the AnyMDx system from the whole blood sample to the molecular diagnostic results. The nucleic acid testing procedure includes the following seamlessly integrated steps: (1) collecting malaria-infected blood into a 1.5 mL microcentrifuge tube containing 1000  $\mu\text{L}$  of lysis buffer and 10  $\mu\text{L}$  of proteinase K, mixing the content thoroughly, and incubating at room temperature for 2 minutes; (2) transferring 180  $\mu\text{L}$  of the lysate into the compact disc through a loading inlet which was sealed after loading; and (3) inserting the compact disc into the AnyMDx instrument. The AnyMDx automatically performs all steps including DNA purification, elution, amplification, and real-time detection. The diagnostic result is shown on an LCD screen or (optionally) on a smartphone through Bluetooth connectivity. Video S1† shows the exemplary sequence of operating the AnyMDx instrument. The turnaround time from sample to answer is less than 40 minutes. Although we could also incorporate the lysis process on the compact disc, an off-chip lysis was

**Table 1** Reagent setup of the LAMP master mix

Component	Concentration	Volume
PCR grade water	1×	7.25 $\mu\text{L}$
Primer sets	—	6.50 $\mu\text{L}$
Isothermal buffer	1×	2.50 $\mu\text{L}$
$\text{MgSO}_4$	7.00 mM	1.75 $\mu\text{L}$
Calcein	25.00 $\mu\text{M}$	0.63 $\mu\text{L}$
$\text{MnCl}_2$	0.75 mM	1.88 $\mu\text{L}$
dNTP mix	1.40 mM	3.50 $\mu\text{L}$
<i>Bst</i> DNA polymerase	0.32 unit per $\mu\text{L}$	1.00 $\mu\text{L}$





**Fig. 4** Location of the LAMP target sequence and priming sites of *Plasmodium falciparum* (Pf: Genbank accession no. AJ276844). The core priming sites of inner/outer primers (F3/B3, F2/B2, and F1c/B1c) with additional priming sites of loop primers (LF/LB) are marked on the sequence.

adopted to ensure the system's compatibility with other sample types (e.g. swab samples).

### 3.2 Passive valve on the microfluidic compact disc

One major challenge in applying microfluidics towards point-of-care testing is the need for peripheral tubing and pumping systems to drive the liquid movement.<sup>33,34</sup> One exception is the centrifugal type microfluidic platform, where the reagent can be preloaded and driven by centrifugal forces.<sup>35</sup> The preloaded reagents rely on passive valves to prevent mixing.<sup>36,37</sup> However, fluid control and separation in the centrifugal platform were challenging because an identical cen-

trifugal force field is applied to all of the liquids on the disc within which a different flow rate is needed.<sup>34,38</sup> In addition, centrifugal force is non-linear in nature and needs rotational frequencies in the range of several thousand revolutions per minute (RPM).<sup>35</sup> The electrical power needed to drive this motion is tremendous.

The microfluidic reagent disc used in the AnyMDx system does not rely on the centrifugal force to move the liquid. Instead, we actuate the DNA-carrying magnetic beads against the stationary reagent droplets. The reagents were preloaded and separated on the microfluidic reagent disc by teeth-shaped passive valves (Fig. 3). The structural pinning effect<sup>39,40</sup> and modified surface tension are the underlying principles that enable the teeth-shaped valves to securely hold the liquid in each chamber. The pinning effect refers to the fact that a sharp bending angle ( $\alpha$ ) of the teeth structure radically increases the liquid/vapor interface area and raises the activation energy, which prevents the fluid from overcoming the barrier (Fig. S3A†).<sup>39</sup> The enhanced surface tension is another important aspect of our passive valve structure. The valve surface was treated with a water-oil repellent to increase the activation barrier by introducing a higher surface tension,<sup>39</sup> which also helps circumvent cross-contamination during sample preparation.

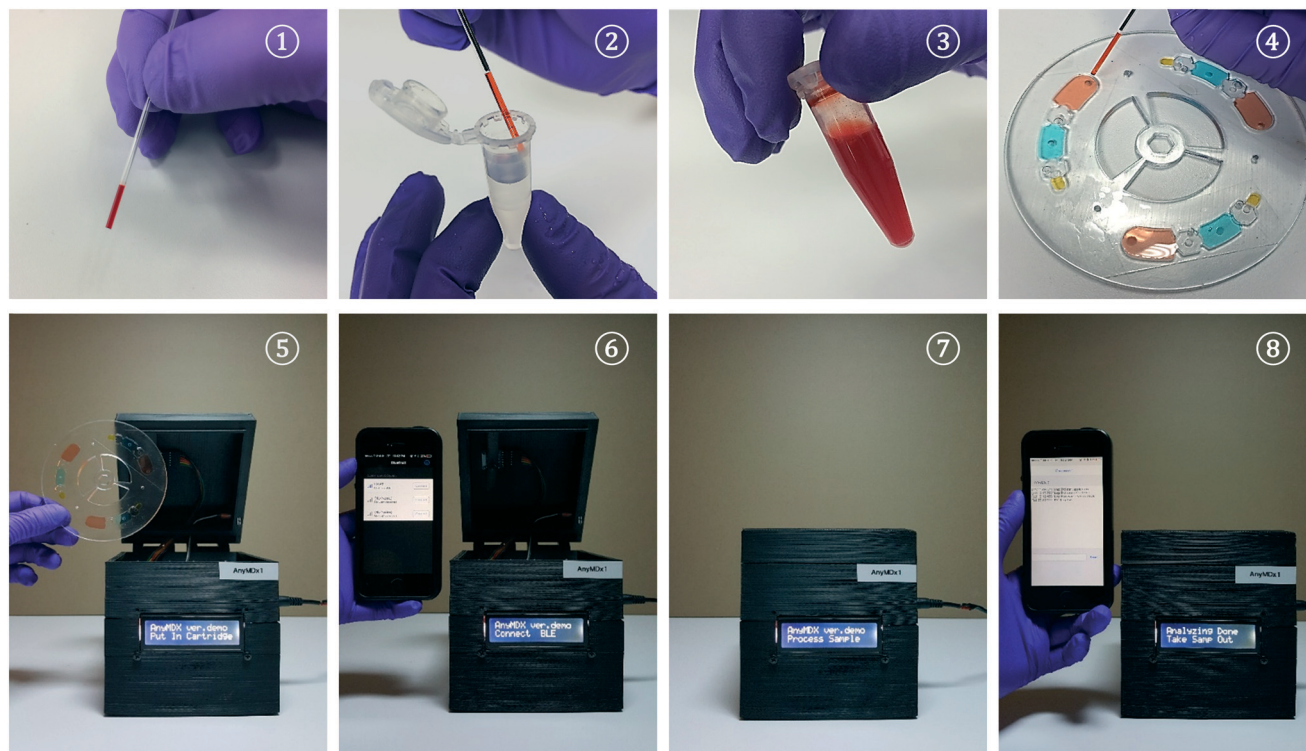


**Fig. 5** Steps for operating the AnyMDx system from sample to answer. 10  $\mu$ L of the whole blood sample was collected into 1 mL of lysis buffer by using a capillary tube, and the lysate was ready to be loaded into the compact disc after incubation at room temperature for 2 minutes (steps 1–3). 180  $\mu$ L of lysate was introduced to the compact disc through the loading inlet which was then sealed by pressure-sensitive adhesive tape (step 4). The sealed compact disc was inserted into the AnyMDx instrument, and the system can be optionally connected to a smartphone user interface (step 5 and 6). When closing the lid, the AnyMDx system automatically performs all assay steps including nucleic acid purification, elution, amplification and real-time detection (step 7). The diagnostic result can be reported within 40 min on a LCD screen or optionally on the smartphone user interface (step 8). Video S1† shows the detailed sequence of operating the AnyMDx system.

To demonstrate the robustness of the passive valve for preventing the reagents from mixing under the harsh mechanical vibration, we performed a drop test on the microfluidic compact disc. Three different colors of food dyes were preloaded into each reagent chamber for visualization of any liquid movement. Each reagent-loading hole was sealed with pressure-sensitive adhesive (PSA) to prevent leakage. The disc was dropped from a height of 20 cm along a guiding rod towards a rigid surface for 25 times. The disc was inspected every five drops with the naked eye to confirm the functionality of the valve. The result showed that the teeth-shaped valve endured 25 consecutive drops without reagents mixing (Fig. S3†). In addition, the robustness of the passive valve was also validated through hand agitation to the microfluidic disc (Video S2†).

### 3.3 Assay validation on the compact disc

To validate the designed LAMP assay and the module level function (fluidic, thermal, mechanical, optical) of the AnyMDx instrument, the LAMP assay in the microfluidic compact disc on the AnyMDx system was compared side by side with a real-time PCR using a purified *P. falciparum* genomic DNA sample. To this end, purified *P. falciparum* genomic DNA (gDNA) was 10-fold serially diluted with Tris-EDTA buffer. LAMP master mix without *P. falciparum* gDNA was used as a no template control (NTC). As shown in Fig. 6A, the assay was firstly validated by a benchtop real-time PCR machine (MJ Research DNA Engine Opticon). A sharp increase in RFU values was observed from three diluted DNA samples, while the negative control showed no increase in RFU values (Fig. 6A). The real-time performance of AnyMDx on the same sample sets is shown in Fig. 6B, which clearly demonstrated a distinguishable fluorescence threshold between positive and negative samples within 30 minutes. In addition, the result of the AnyMDx system was quantitative although the standard deviations are higher for low concentration sam-

ples. An inversely proportional relationship between the threshold time and the DNA concentrations ( $R^2 = 0.9998$ ) was observed (Fig. 6B, inset). Note that AnyMDx has a linear region from 0.01× to 1×, while the real-time PCR machine saturates at 1× concentration. This discrepancy might be due to the dynamic range differences in the optical detectors and the thermal coupling efficiency in these two systems.

To further evaluate if the amplicons were specifically from the designed targets, we performed gel electrophoresis analysis of the amplicons in 2% agarose gel. As shown in Fig. 6C, the LAMP amplicons showed a clear ladder-like pattern with multiple bands of different molecular sizes due to its inverted-repeat structures.<sup>41</sup> More specifically, the length of the observed bands corresponds to the integral times of the target sequence (213 bp), indicating that the amplified products were specific for the target sequence. In addition, strong green emission (implying positive reactions) can be easily recognized by the naked eye in the PCR tube under blue LED illumination in the dark environment (Fig. 6D). From these results, we successfully verified the LAMP assay against *P. falciparum* genomic DNA and the modular function of the AnyMDx system.

### 3.4 Integrated sample preparation on the compact disc

High-quality nucleic acid sample preparation is the bottleneck for most “sample-in-answer-out” molecular analysis.<sup>42</sup> Before we prepared the sample on the reagent compact disc, the pH-switchable magnetic bead-based method for DNA isolation was validated first in test tubes from the blood sample using the same reagents as on the reagent compact disc. Successful amplification of the tube-extracted DNA samples confirmed the effectiveness of the magnetic bead-based method (Fig. S4†). Afterward, we evaluated sample preparation in the reagent compact disc and the compatibility of the purified DNA with the subsequent LAMP assay. To test the DNA extraction efficiency on the reagent compact disc, we examined

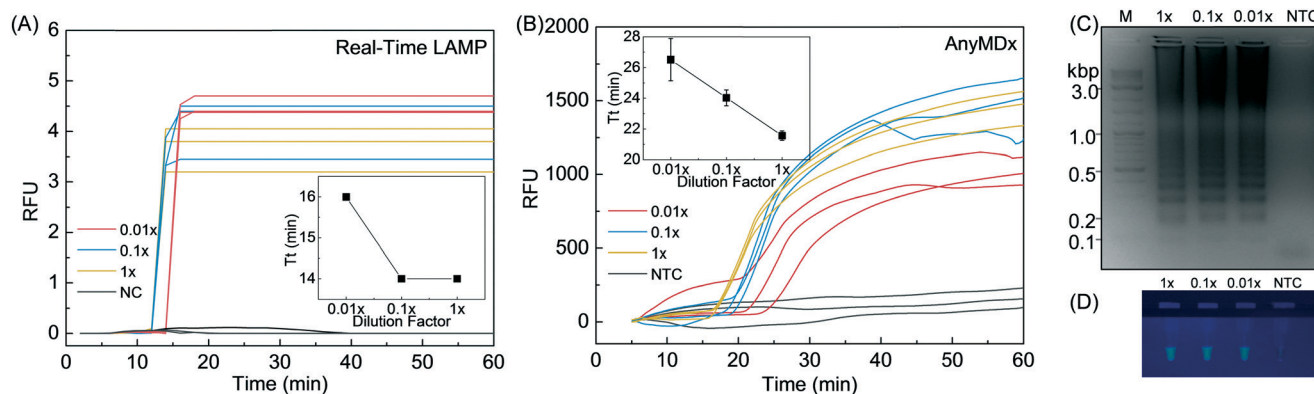


**Fig. 6** Validation of the LAMP assay and the AnyMDx instrument with laboratory purified DNA samples. (A) Benchmarking amplification curves obtained from the real-time PCR machine. 1×, 0.1×, and 0.01× denote the dilution factors of the *P. falciparum* DNA samples (NTC: no template controls,  $T_t$ : threshold time). (B) The amplification profiles acquired from the AnyMDx instrument. (C) Gel-electrophoresis analysis on a 2% agarose gel. The amplicons show a clear ladder-like pattern, the length of which verifies the LAMP assay's specificity against *P. falciparum*. (D) Emission visualized under the blue LED ( $\lambda = 488$  nm) illumination for various positive and negative samples.

*P. falciparum* infected blood samples of different parasitemias (0.2%, 0.02%, and 0.002%, prepared by dilution with healthy blood at 45% hematocrit). The infected blood samples were directly lysed in the collection tubes before loading into the reagent compact disc (Fig. 3B). The following DNA binding, purification, elution, and the amplification were automatically carried out by the AnyMDx system (Fig. 3C). As shown in Fig. 7, the real-time amplification data for various parasitemias showed a clear quantitative trend, as compared to the lack of amplification signals in the negative control. Although quantitative analysis is not always required for point-of-care applications, it is valuable in many situations, for example, in determining the effectiveness of anti-malarial therapy for malaria patients.<sup>43</sup> These results fully verified that the AnyMDx system could work in a “sample-in-answer-out” fashion by seamlessly integrating high-quality DNA preparation and real-time amplification into a single reagent compact disc.

### 3.5 Assay sensitivity

To evaluate the diagnostic sensitivity<sup>44</sup> of the AnyMDx system for analyzing the whole blood samples, various parasitemias of *P. falciparum*-infected blood (from 2% to 0.00002%, and 2% parasitemia corresponds to ~60 000 parasites per  $\mu\text{L}$ ) were prepared by diluting with fresh human RBCs at 45% hematocrit. In addition, the master mix (Table 1) without target DNA as well as the healthy RBCs (hRBC) were used as negative controls. To evaluate the test-to-test variations, each whole blood sample was examined independently three times. As shown in Fig. 8, the amplification curves of the infected RBC samples show clear exponential increases in fluorescence, while those of the negative controls (master mix and hRBC) show no amplification. The amplification threshold time was inversely proportional to the parasitemia

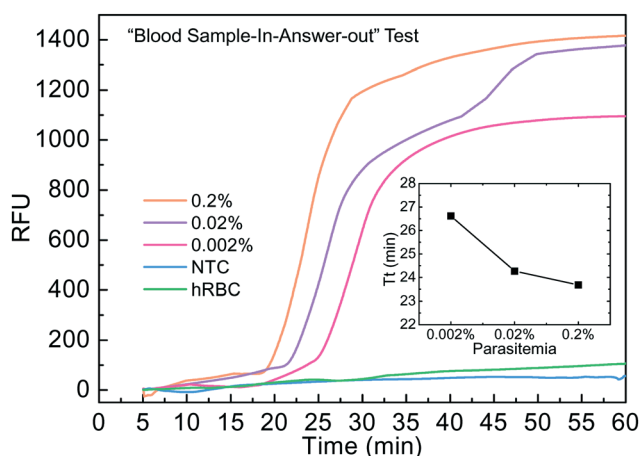


Fig. 7 Validation of the AnyMDx system from the whole blood sample to the amplification result with integrated sample preparation on the compact disc. The % value represents the parasitemia of the infected RBCs (hRBC: healthy RBCs, NTC: no template controls,  $T_t$ : threshold time).

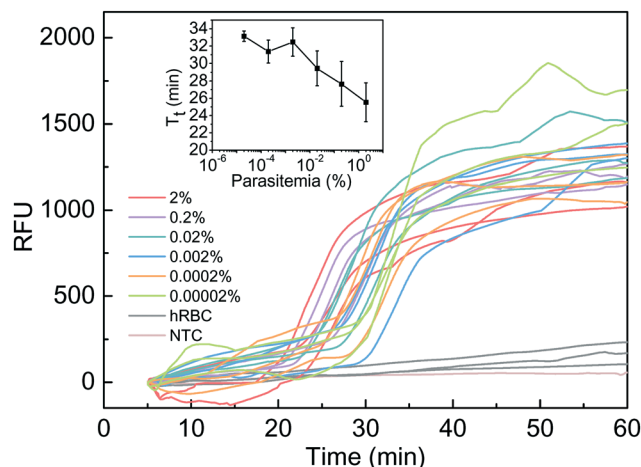


Fig. 8 AnyMDx sensitivity for detecting *P. falciparum* infected blood samples. Amplification curves for various infected blood samples of different parasitemias. The inversely proportional relationship between the amplification threshold time and the parasitemia confirms the quantitative ability of the AnyMDx system. A detection limit of ~0.6 parasite per  $\mu\text{L}$  (i.e. 0.00002% parasitemia) against *P. falciparum* was successfully achieved.

(inset of Fig. 8). We observed high standard deviation values in the inset of Fig. 8. This is because conversion from parasitemia to DNA copy numbers is not exactly linear when a sample preparation process is involved, a known challenge even with the commercial real-time PCR.

Parasite DNA in the blood sample at 0.00002% parasitemia could be successfully detected and quantified, which corresponded to a detection limit of ~0.6 parasite per  $\mu\text{L}$ . Since we only used 180  $\mu\text{L}$  out of a total of 1020  $\mu\text{L}$  of lysate as the input to the reagent compact disc (Fig. 3), a lower detection limit (~0.1 parasite per  $\mu\text{L}$ ) could be achieved if all lysate volumes were used (requiring a disc redesign). The detection limit of ~0.6 parasite per  $\mu\text{L}$  of the AnyMDx is comparable to the benchtop real-time PCR test (~0.7 parasite per  $\mu\text{L}$ <sup>45</sup>) and to the benchtop LAMP test (~2 parasites per  $\mu\text{L}$ <sup>9</sup>). This level of sensitivity is necessary for detecting the early-stage asymptomatic parasite carriers of low parasite densities,<sup>9,46</sup> which are often missed by either the immunoassay based rapid diagnostic tests (RDTs, ~100 parasites per  $\mu\text{L}$ <sup>7</sup>) or microscopy (~30–50 parasites per  $\mu\text{L}$ <sup>7,11</sup>). Thus, the AnyMDx system is able to deliver ultrasensitive and quantitative molecular answers for malaria infections in remote settings without supporting infrastructures.

### 3.6 Cost analysis

The greatest advantage of the molecular test is their ability to detect extremely low-level malaria infections, which are often challenging for microscopy and RDTs. Nevertheless, the greatest hurdle for deploying a molecular test in resource-limited areas is its relatively high cost and the infrastructure investment. The AnyMDx system aimed to address this issue



by delivering a sensitive malaria molecular test in a cost-effective way. The prototype AnyMDx instrument presented in this work could be built for a total amount of ~\$176 (see Table S2† for cost breakdown). The disposable reagent compact disc (including the sample preparation and the amplification reagents) costs ~\$1.14 per each test (Table S3†). Note that this cost analysis is only carried out to provide a ballpark figure to the interested researchers who want to replicate the system. Reduced cost for scaled manufacturing, increased cost for medical device regulation, and licensing cost is not included in this analysis since this is beyond the scope of this study. The low cost of this sensitive molecular test provides a great opportunity for the field applications of this mobile molecular diagnostic system. Moreover, the manufacturing of the AnyMDx instrument is highly scalable in a cost-effective way. The AnyMDx system could be easily reproduced within a day in ordinary lab settings. The instrument-to-instrument variation was small enough to deliver the same quality of quantitative molecular analysis (Fig. S5†). As a result, we envision that the AnyMDx would enable cost-effective malaria molecular diagnosis in resource-limited regions by decreasing the cost, increasing the ease of use, and maintaining high sensitivity.

## 4 Conclusions

We developed a field-deployable mobile molecular diagnostic system for rapid and accurate diagnosis of malaria infection in resource-limited areas at the point of need. The AnyMDx system seamlessly integrated all nucleic acid testing steps from sample preparation to real-time amplification and detection. The standalone and user-friendly system works in an “insert-and-test” fashion and could specifically detect *P. falciparum* species in 40 minutes from a whole blood sample. The sensitivity against *P. falciparum* was ~0.6 parasite per  $\mu\text{L}$ , which is important for identifying asymptomatic parasite carriers who will otherwise be missed by microscopy or RDT.<sup>7,12,47</sup> The cost-effective system allows for the deployment of benchtop-quality malaria nucleic acid testing into the remote areas for malaria elimination. Moreover, the modular design of a separate reagent compact disc and a durable analyzer makes the system versatile. As a platform technology, the AnyMDx design should create a new paradigm of molecular diagnosis towards a variety of infectious diseases at the point of care.

## Acknowledgements

This project was partly supported by the Penn State CTSI Grant (UL Tr000127) from the National Center for Advancing Translational Sciences, National Institutes of Health. The content is solely the responsibility of the authors and does not necessarily represent the official views of the NIH. This project was also supported by Penn State Engineering for Innovation & Entrepreneurship (ENGINE) Grant. We express our

gratitude to Xiaolian Li for providing malaria samples and to Zhoufa Chen and Dr. Xiaonan Yang for fruitful discussions.

## References

- 1 A. Enayati and J. Hemingway, *Annu. Rev. Entomol.*, 2010, 55, 569–591.
- 2 B. Greenwood and T. Mutabingwa, *Nature*, 2002, 415, 670–672.
- 3 WHO, *World Malaria Report 2015*, 2015, pp. 1–255.
- 4 S. Bhatt, D. J. Weiss, E. Cameron, D. Bisanzio, B. Mappin, U. Dalrymple, K. E. Battle, C. L. Moyes, A. Henry, P. A. Eckhoff, E. A. Wenger, O. Briet, M. A. Penny, T. A. Smith, A. Bennett, J. Yukich, T. P. Eisele, J. T. Griffin, C. A. Fergus, M. Lynch, F. Lindgren, J. M. Cohen, C. L. J. Murray, D. L. Smith, S. I. Hay, R. E. Cibulskis and P. W. Gething, *Nature*, 2015, 526, 207–211.
- 5 A. F. Vallejo, N. L. Martinez, I. J. Gonzalez, M. Arevalo-Herrera and S. Herrera, *PLoS Neglected Trop. Dis.*, 2015, 9, e3453.
- 6 S. S. Modak, C. A. Barber, E. Geva, W. R. Abrams, D. Malamud and Y. S. Ongagna, *Infect. Dis.*, 2016, 9, 1–9.
- 7 C. Wongsrichanalai, M. J. Barcus, S. Muth, A. Sutamihardja and W. H. Wernsdorfer, *Am. J. Trop. Med. Hyg.*, 2007, 77, 119–127.
- 8 H. Hopkins, I. J. Gonzalez, S. D. Polley, P. Angutoko, J. Ategeka, C. Asiimwe, B. Agaba, D. J. Kyabayinze, C. J. Sutherland, M. D. Perkins and D. Bell, *J. Infect. Dis.*, 2013, 208, 645–652.
- 9 B. Aydin-Schmidt, W. P. Xu, I. J. Gonzalez, S. D. Polley, D. Bell, D. Shakely, M. I. Msellem, A. Bjorkman and A. Martensson, *PLoS One*, 2014, 9, e103905.
- 10 T. Leslie, A. Mikhail, I. Mayan, M. Anwar, S. Bakhtash, M. Nader, C. Chandler, C. J. M. Whitty and M. Rowland, *BMJ [Br. Med. J.]*, 2012, 345, e4389.
- 11 C. W. Pirnstill and G. L. Cote, *Sci. Rep.*, 2015, 5, 13368.
- 12 L. Wu, L. L. van den Hoogen, H. Slater, P. G. T. Walker, A. C. Ghani, C. J. Drakeley and L. C. Okell, *Nature*, 2015, 528, S86–S93.
- 13 U. Morris, M. Khamis, B. Aydin-Schmidt, A. K. Abass, M. I. Msellem, M. H. Nassor, I. J. Gonzalez, A. Martensson, A. S. Ali, A. Bjorkman and J. Cook, *Malar. J.*, 2015, 14, 1–6.
- 14 E. T. Han, R. Watanabe, J. Sattabongkot, B. Khuntirat, J. Sirichaisinthop, H. Iriko, L. Jin, S. Takeo and T. Tsuboi, *J. Clin. Microbiol.*, 2007, 45, 2521–2528.
- 15 S. D. Polley, Y. Mori, J. Watson, M. D. Perkins, I. J. Gonzalez, T. Notomi, P. L. Chiodini and C. J. Sutherland, *J. Clin. Microbiol.*, 2010, 48, 2866–2871.
- 16 M. Safavieh, M. K. Kanakasabapathy, F. Tarlan, M. U. Ahmed, M. Zourob, W. Asghar and H. Shafiee, *ACS Biomater. Sci. Eng.*, 2016, 2, 278–294.
- 17 N. Tomita, Y. Mori, H. Kanda and T. Notomi, *Nat. Protoc.*, 2008, 3, 877–882.
- 18 M. Goto, E. Honda, A. Ogura, A. Nomoto and K. I. Hanaki, *BioTechniques*, 2009, 46, 167–172.
- 19 T. Notomi, Y. Mori, N. Tomita and H. Kanda, *J. Microbiol.*, 2015, 53, 1–5.

- 20 J. Kim, M. Johnson, P. Hill and B. K. Gale, *Integr. Biol.*, 2009, **1**, 574–586.
- 21 F. B. Myers, R. H. Henrikson, J. Bone and L. P. Lee, *PLoS One*, 2013, **8**, e70266.
- 22 S. C. Liao, J. Peng, M. G. Mauk, S. Awasthi, J. Z. Song, H. Friedman, H. H. Bau and C. C. Liu, *Sens. Actuators, B*, 2016, **229**, 232–238.
- 23 C. C. Liu, M. G. Mauk, R. Hart, M. Bonizzoni, G. Y. Yan and H. H. Bau, *PLoS One*, 2012, **7**, e42222.
- 24 S. Choi, *Biotechnol. Adv.*, 2016, **34**, 321–330.
- 25 G. Abel, *Expert Rev. Mol. Diagn.*, 2015, **15**, 853–855.
- 26 W. E. Jung, J. Han, J. W. Choi and C. H. Ahn, *Microelectron. Eng.*, 2015, **132**, 46–57.
- 27 K. Yang, H. Peretz-Soroka, Y. Liu and F. Lin, *Lab Chip*, 2016, **16**, 943–958.
- 28 J. Hu, X. Y. Cui, Y. Gong, X. Y. Xu, B. Gao, T. Wen, T. J. Lu and F. Xu, *Biotechnol. Adv.*, 2016, **34**, 305–320.
- 29 W. Trager and J. B. Jensen, *Science*, 1976, **193**, 673–675.
- 30 T. Ponnudurai, J. H. Meuwissen, A. D. Leeuwenberg, J. P. Verhave and A. H. Lensen, *Trans. R. Soc. Trop. Med. Hyg.*, 1982, **76**, 242–250.
- 31 C. Lambros and J. P. Vanderberg, *J. Parasitol.*, 1979, **65**, 418–420.
- 32 K. Y. Lien, C. J. Liu, Y. C. Lin, P. L. Kuo and G. B. Lee, *Microfluid. Nanofluid.*, 2009, **6**, 539–555.
- 33 A. W. Martinez, S. T. Phillips, G. M. Whitesides and E. Carrilho, *Anal. Chem.*, 2010, **82**, 3–10.
- 34 L. X. Kong, K. Parate, K. Abi-Samra and M. Madou, *Microfluid. Nanofluid.*, 2015, **18**, 1031–1037.
- 35 M. Madou, J. Zoval, G. Y. Jia, H. Kido, J. Kim and N. Kim, *Annu. Rev. Biomed. Eng.*, 2006, **8**, 601–628.
- 36 J. M. Park, Y. K. Cho, B. S. Lee, J. G. Lee and C. Ko, *Lab Chip*, 2007, **7**, 557–564.
- 37 R. Gorkin, J. Park, J. Siegrist, M. Amasia, B. S. Lee, J. M. Park, J. Kim, H. Kim, M. Madou and Y. K. Cho, *Lab Chip*, 2010, **10**, 1758–1773.
- 38 R. Burger, P. Reith, V. Akujobi and J. Ducree, *Microfluid. Nanofluid.*, 2012, **13**, 675–681.
- 39 L. C. Gao and T. J. McCarthy, *Langmuir*, 2006, **22**, 6234–6237.
- 40 D. Oner and T. J. McCarthy, *Langmuir*, 2000, **16**, 7777–7782.
- 41 T. Notomi, H. Okayama, H. Masubuchi, T. Yonekawa, K. Watanabe, N. Amino and T. Hase, *Nucleic Acids Res.*, 2000, **28**, e63.
- 42 A. M. Foudeh, T. F. Didar, T. Veres and M. Tabrizian, *Lab Chip*, 2012, **12**, 3249–3266.
- 43 M. A. Lee, C. H. Tan, L. T. Aw, C. S. Tang, M. Singh, S. H. Lee, H. P. Chia and E. P. H. Yap, *J. Clin. Microbiol.*, 2002, **40**, 4343–4345.
- 44 A. J. Saah and D. R. Hoover, *Ann. Intern. Med.*, 1997, **126**, 91–94.
- 45 F. Perandin, N. Manca, A. Calderaro, G. Piccolo, L. Galati, L. Ricci, M. C. Medici, M. C. Arcangeletti, G. Snounou, G. Dettori and C. Chezzi, *J. Clin. Microbiol.*, 2004, **42**, 1214–1219.
- 46 H. C. Slater, A. Ross, A. L. Ouedraogo, L. J. White, C. Nguon, P. G. T. Walker, P. Ngor, R. Aguas, S. P. Silal, A. M. Dondorp, P. La Barre, R. Burton, R. W. Sauerwein, C. Drakeley, T. A. Smith, T. Bousema and A. C. Ghani, *Nature*, 2015, **528**, S94–S101.
- 47 B. Moonen, J. M. Cohen, R. W. Snow, L. Slutsker, C. Drakeley, D. L. Smith, R. R. Abeyasinghe, M. H. Rodriguez, R. Maharaj, M. Tanner and G. Targett, *Lancet*, 2010, **376**, 1592–1603.